ASXL1 mutations accelerate bone marrow fibrosis via EGR1-TNFA axis-mediated neoplastic fibrocyte generation in myeloproliferative neoplasms

Zhongxun Shi,[1*] Jinqin Liu,[1*] Yingying Zhao,[2*] Lin Yang,[1] Yanan Cai,[1] Peihong Zhang,[1] Zefeng Xu,[1] Tiejun Qin,[1] Shiqiang Qu,[1] Lijuan Pan,[1] Junying Wu,[1] Xin Yan,[1] Zexing Li,[2] Wenjun Zhang,[1] Yiru Yan,[1] Huijun Huang,[1] Gang Huang,[3#] Bing Li,[1#] Xudong Wu[1,2#] and Zhijian Xiao[1#]

[1]State Key Laboratory of Experimental Hematology, National Clinical Research Center for Blood Diseases, Haihe Laboratory of Cell Ecosystem, Institute of Hematology & Blood Diseases Hospital, Chinese Academy of Medical Sciences & Peking Union Medical College, Tianjin, China; [2]The Province and Ministry Co-sponsored Collaborative Innovation Center for Medical Epigenetics, Department of Cell Biology, Tianjin Medical University, Tianjin, China and [3]Divisions of Pathology and Experimental Hematology and Cancer Biology, Cincinnati Children's Hospital Medical Center, Cincinnati, OH, USA

ZXS, JQL and YYZ. contributed equally as co-first authors.
#ZJX, XDW, BL and GH contributed equally as co-senior authors.

Correspondence:
Z. Xiao
zjxiao@ihcams.ac.cn
X. Wu
wuxudong@tmu.edu.cn
B. Li
libing@ihcams.ac.cn
G. Huang
gang.huang@cchmc.org

Received: November 7, 2021.
Accepted: June 28, 2022.
Early view: August 25, 2022.

https://doi.org/10.3324/haematol.2021.280320

Abstract

Apart from the central role of the activated JAK/STAT signaling pathway, *ASXL1* mutations are the most recurrent additional mutations in myeloproliferative neoplasms and occur much more commonly in myelofibrosis than in essential thrombocythemia and polycythemia vera. However, the mechanism of the association with *ASXL1* mutations and bone marrow fibrosis remains unknown. Here, integrating our own data from patients with myeloproliferative neoplasms and a hematopoietic-specific *Asxl1* deletion/*Jak2*^{V617F} mouse model, we show that *ASXL1* mutations are associated with advanced myeloproliferative neoplasm phenotypes and onset of myelofibrosis. *ASXL1* mutations induce skewed monocyte/macrophage and neoplastic monocyte-derived fibrocyte differentiation, consequently they enhance inflammation and bone marrow fibrosis. Consistently, the loss of *ASXL1* and *JAK2*^{V617F} mutations in hematopoietic stem and progenitor cells leads to enhanced activation of polycomb group target genes, such as *EGR1*. The upregulation of *EGR1*, in turn, accounts for increased hematopoietic stem and progenitor cell commitment to the monocyte/macrophage lineage. Moreover, *EGR1* induces the activation of *TNFA* and thereby further drives the differentiation of monocytes to fibrocytes. Accordingly, combined treatment with a TNFR antagonist and ruxolitinib significantly reduces fibrocyte production *in vitro*. Altogether, these findings demonstrate that *ASXL1* mutations accelerate fibrocyte production and inflammation in myeloproliferative neoplasms via the EGR1-TNFA axis, explaining the cellular and molecular basis for bone marrow fibrosis and the proof-of-concept for anti-fibrosis treatment.

Introduction

Myeloproliferative neoplasms (MPN) are malignant clonal diseases originating from hematopoietic stem cells, characterized by the proliferation of one or more myeloid lineages and an increasing risk of transformation to acute myeloid leukemia.[1] Primary myelofibrosis (PMF) is the subtype with the worst prognosis.[2] Moreover, approximately 15% of patients with essential thrombocythemia (ET) or polycythemia vera (PV) develop post-ET/PV MF over time, which is similar to PMF in treatment and outcome.[1] Somatic mutations in *Janus kinase 2* (*JAK2*), *calreticulin* (*CALR*), or *myeloproliferative leukemia protein* (*MPL*) are regarded as driver mutations that activate the JAK/STAT signaling pathway and are essential for the MPN phenotype.[3-5] *JAK2*^{V617F} is the most common driver mutation and is present in more than 95% of cases of PV and more than 50% of ET and MF (including PMF and post-ET/PV MF) patients.[2]

Although inappropriate JAK/STAT pathway activation exists in most MF patients, the JAK1/JAK2 inhibitor ruxolitinib has a limited effect on reversing fibrosis grades in MF patients.[6] Meanwhile, there are reports of several animal models with *Jak2*^{V617F} which induce PV or ET-like phenotypes while MF is rare.[7-9] Besides driver mutations, additional mutations are common in MF patients,[10,11] and the mouse models with concomitant *Jak2*^{V617F} and *Ezh2*, *Tet2* or *Dnmt3a* loss showed accelerated MF as well. However, the mechanisms are not fully delineated.[12-14]

ASXL1 mutations are the most recurrent nondriver mutations in MF and are much more common in PV and ET patients.[10,11] As one of the mammalian homologs of the *Drosophila Asx*,[15] polycomb group (PcG) genes, *ASXL1* acts as an essential cofactor for the nuclear deubiquitinase BRCA1-Associated Protein 1 (BAP1)[16,17] and as a critical mediator of Polycomb Repressive Complex 2 (PRC2),[18] participating in the epigenetic control of gene expression. Frameshift and nonsense mutations are the major types of *ASXL1* mutation, resulting in C-terminal truncation and usually loss of *ASXL1* expression.[18] Wild-type ASXL1 plays an essential role in normal hematopoiesis. *Asxl1* knockout mice show impaired hematologic progenitor differentiation and development of myelodysplasia and myelodysplastic syndrome/MPN.[19] In J*ak2*^{V617F} mice, heterozygous knockout of *Asxl1* in germline accelerates MF progression,[20] while how ASXL1 loss results in transcription deregulation and aberrant lineage differentiation in MPN remains poorly understood.

In this study, we analyzed the clinical characteristics of *ASXL1* mutations in MF patients and generated hematopoietic-specific *Asxl1* knockout and J*ak2*^{V617F} knockin mouse models. Our data showed that *ASXL1* mutations could promote monocyte/macrophage-mediated inflammation and neoplastic monocyte-derived fibrocyte-induced bone marrow (BM) fibrosis by activating the EGR1-TNFA axis in both *ASXL1*-mutated MF patients and *Asxl1* knockout/J*ak2*^{V617F} mice, offering novel potential therapeutic strategies for anti-fibrosis treatment.

Methods

Patients and animals

Three hundred and two consecutive MF patients were investigated in this study. Diagnoses were classified according to 2016 World Health Organization (WHO) MPN definitions.[21] All patients gave written informed consent compliant with the Declaration of Helsinki. Studies involving medical records and human tissues were approved by the Ethics Committee of the blood disease hospital, Chinese Academy of Medical Sciences & Peking Union Medical College. For mouse model studies, cre-inducible *Jak2*$^{LSL\ V617F/+}$ mice, *Asxl1*$^{flox/flox}$ mice and hematopoietic-specific *Vav1*-Cre transgenic mice were used. All mice were on a C57BL/6 background. Details are contained in the *Online Supplementary Methods*. The experimental protocols were approved by the Institutional Animal Care and Use Committee of State Key Laboratory of Experimental Hematology.

In vitro monocyte/macrophage differentiation assay

Murine BM was isolated and enriched for c-kit using CD117 MicroBeads (Miltenyi) and separated using an AutoMACS Pro separator (Miltenyi). BM c-kit$^+$ cells were plated in methylcellulose medium (Methocult M3234, Stem Cell Technologies) supplemented with mouse interleukin (IL)-3 (Peprotech, 10 ng/mL) for 1×10^4 cells per well. After 8 days, colonies were counted, then isolated, pooled, and resuspended in phosphate-buffered saline, and stained with F4/80 antibodies (Biolegend, 123115) for flow cytometric analysis on a FACS Canto II flow cytometer (BD Biosciences). Additionally, Wright-Giemsa-stained cytospin smears were prepared for morphological analysis.

In vitro fibrocyte differentiation assay and quantification

Murine BM nucleated cells or patients' BM mononuclear cells were resuspended in conditions that promote the differentiation of monocytes to fibrocytes.[22,23] Cells were cultured in 24-well tissue culture plates with 5×10^5 cells/500 μL. After 5 days, immunofluorescence staining was performed to identify fibrocytes. Details of the protocols are provided in the *Online Supplementary Methods*.

Immunohistochemical and image quantification of patients' samples

Bone marrow biopsy sections were dewaxed, rehydrated and retrieved. Sections were blocked in 10% donkey/10% goat serum or 10% donkey serum and then incubated with primary antibodies overnight followed by secondary staining. Next, AutoFluo Quencher (Applygen) was applied to quench autofluorescence. Finally, glass coverslips were mounted onto the slides using Mounting Medium with DAPI (Abcam). Images were captured by confocal microscopy (PerkinElmer UltraVIEW VoX system) and quantified using Fiji-ImageJ software. Details of the protocols are contained in the *Online Supplementary Methods*.

Gene-expression profiling and bioinformatics analysis

Murine BM c-kit$^+$ cells were enriched for bulk RNA sequencing, assay for transposase-accessible chromatin (ATAC) with sequencing and chromatin immunoprecipitation (ChIP) sequencing. Detailed protocols are contained in the *Online Supplementary Methods*.

A more detailed description of the methods is published in the *Online Supplementary Appendix*.

Results

ASXL1 mutations are associated with severe disease phenotypes in patients with myelofibrosis

To determine the clinical impact of *ASXL1* mutations on MF patients, we analyzed data from 302 MF patients in our single center; 250 (82.8%) patients displayed driver mutations, including 174 (57.6%) $JAK2^{V167F}$, 63 (20.9%) *CALR*, and 13 (4.3%) *MPL* mutations (*Online Supplementary Figure S1A*). 98 (32.5%) patients harbored *ASXL1* mutations. Figure 1A shows the landscape of localizations and types of *ASXL1* mutation. Frameshift mutations were the most common mutation type (N=50, 51.0%) followed by nonsense (N=46, 46.9%) and missense mutations (N=2, 2.0%).

Figure 1B-D and *Online Supplementary Table S1* summarize the clinical and laboratory characteristics of MF patients according to *ASXL1* mutations. In this cohort, *ASXL1* mutations were correlated with lower hemoglobin levels, higher monocyte counts, increasing $CD34^+$ cells in peripheral blood (PB), larger spleen sizes, and higher MF grades, consistent with prior studies.[10] Similar results were also found in the driver mutation positive ($driver^{MT}$) cohort (N=250) (Figure 1E-G, *Online Supplementary Table S2*). We next analyzed the co-mutations in MF patients with or without *ASXL1* mutations. Considering the total cohort, compared with *ASXL1* wildtype ($ASXL1^{WT}$) patients, *ASXL1*-mutated ($ASXL1^{MT}$) patients more commonly had *CALR*, *KRAS*, and *ZRSR2* mutations (*Online Supplementary Figure S1B*), while considering the $driver^{MT}$ cohort, *CALR* and *NRAS* mutations were more frequent in the $ASXL1^{MT}$ patients than in the $ASXL1^{WT}$ patients (*Online Supplementary Figure S1C*). Altogether, these data suggest that *ASXL1* mutations are associated with severe disease phenotypes in MF patients.

Asxl1 deletion is associated with enhanced extramedullary hematopoiesis in the spleen and onset of bone marrow fibrosis in $Asxl1^{-/-}Jak2^{V617F/+}$ mice

To further address the consequences of *ASXL1* mutations on MPN *in vivo*, we utilized *Vav1*-Cre mice, $Asxl1^{flox/flox}$ and $Jak2^{V617F/+}$ knockin alleles to achieve hematopoietic cell-specific $Jak2^{V617F/+}/Asxl1^{flox/flox}$ ($Asxl1^{-/-}Jak2^{VF}$), $Jak2^{V617F/+}$ ($Jak2^{VF}$), and $Asxl1^{flox/flox}$ ($Asxl1^{-/-}$) mice. In control with wild-type (WT) mice, both $Asxl1^{-/-}Jak2^{VF}$ and $Jak2^{VF}$ mice developed erythrocytosis and died of thrombosis at an early stage of the disease (Figure 2A, *Online Supplementary Figure S2A, B*). Compared with age-matched $Jak2^{VF}$ mice, $Asxl1^{-/-}Jak2^{VF}$ mice showed lower white blood cell, lymphocyte and platelet counts, and higher monocyte counts in PB (Figure 2A). Furthermore, the percentages of $c\text{-}kit^+$ cells in PB were significantly increased in $Asxl1^{-/-}Jak2^{VF}$ mice compared to other genotypes (Figure 2B).

Consistent with PB findings, $Asxl1^{-/-}Jak2^{VF}$ mice showed comparable erythropoiesis in BM and spleens (*Online Supplementary Figure S2C*), and a decreased proportion of B lymphocytes ($B220^+$) in BM compared with $Jak2^{VF}$ mice (*Online Supplementary Figure S2D*). Analysis of the hematopoietic stem and progenitor cell (HSPC) compartment revealed comparable percentages of $Lin^-Scal1^+c\text{-}kit^+$ (LSK) cells, granulocyte/macrophage progenitors, and megakaryocyte/erythroid progenitors in the BM of $Asxl1^{-/-}Jak2^{VF}$ and $Jak2^{VF}$ mice (Figure 2C, *Online Supplementary Figure S2E*), whereas in the comparison with $Jak2^{VF}$ mice, the proportions of granulocyte/macrophage progenitors and megakaryocyte/erythroid progenitors were significantly higher in spleens of $Asxl1^{-/-}Jak2^{VF}$ (Figure 2D, *Online Supplementary Figure S2E*), in line with the increased spleen weights of $Asxl1^{-/-}Jak2^{VF}$ mice (Figure 2E). We next performed methylcellulose colony-forming assays to verify the effect of *Asxl1* deletion on HSPC functions in $Asxl1^{-/-}Jak2^{VF}$ mice. Colony-forming capacities of nucleated cells were enhanced in spleen cells from $Asxl1^{-/-}Jak2^{VF}$ mice compared with those of other genotypes, whereas there was no difference in BM colony-forming capacity between mice of different genotypes (*Online Supplementary Figure S3A, B*), indicating more activated extramedullary hematopoiesis in the spleens of $Asxl1^{-/-}Jak2^{VF}$ mice.

BM histology analysis revealed typical features of MPN with trilineage hyperplasia, especially increased megakaryocytes and atypia in both $Jak2^{VF}$ and $Asxl1^{-/-}Jak2^{VF}$ mice (Figure 3). Interestingly, reticulin and collagen fiber infiltration was present in $Asxl1^{-/-}Jak2^{VF}$ mice at 16 weeks of age, but not in other genotypes (Figure 3). Additionally, $Asxl1^{-/-}Jak2^{VF}$ and $Jak2^{VF}$ spleen specimens exhibited effacement of normal splenic architecture and extramedullary hematopoiesis was more obvious in $Asxl1^{-/-}Jak2^{VF}$ mice relative to $Jak2^{VF}$ mice (Figure 3, *Online Supplementary Figure S3C*).

To further confirm that these findings are cell-autonomous, we transplanted BM nucleated cells from $Asxl1^{-/-}Jak2^{VF}$, $Jak2^{VF}$, $Asxl1^{-/-}$ and WT mice into lethally irradiated recipients (*Online Supplementary Figure S4A*). The survival of recipients of cells from $Asxl1^{-/-}Jak2^{VF}$ mice was worse than that of mice transplanted with cells of other genotypes (*Online Supplementary Figure S4B*). At 24 weeks after transplantation, $Asxl1^{-/-}Jak2^{VF}$ –cell recipients gradually developed monocytosis and thrombocytopenia compared with $Jak2^{VF}$–cell recipients (*Online Supplementary Figure S4C*). Meanwhile, the proportions of $c\text{-}kit^+$ cells in PB were significantly higher in $Asxl1^{-/-}Jak2^{VF}$ recipients (*Online Supplementary Figure S4D*). Additionally, HSPC compartment analysis showed increased myeloid progenitors ($Lin^-Sca1^-c\text{-}kit^+$) in spleens, not in BM of recipients of $Asxl1^{-/-}Jak2^{VF}$ cells in comparison with $Jak2^{VF}$-cell recipients (*Online Supplementary Figure S4E*), despite comparable spleen weights in these two groups (*Online Supplementary Figure S4F*). Histological analysis revealed increased reticulin and collagen fibers in BM and enhanced extramedullary hematopoiesis in spleens of recipients of $Asxl1^{-/-}Jak2^{VF}$ cells compared with $Jak2^{VF}$–cell

recipients at 38-40 weeks after transplantation (*Online Supplementary Figure S4G*).

Taken together, our findings in *Asxl1*$^{-/-}$*Jak2*^{VF} mice are consistent with clinical findings in *ASXL1*^{MT} MF patients, indicating that *ASXL1* mutations are associated with MPN disease progression.

Skewed inflammatory monocyte/macrophage differentiation in *ASXL1*^{MT} myelofibrosis patients and *Asxl1*$^{-/-}$*Jak2*^{VF} mice

The overproduction of inflammatory cytokines is a hallmark feature in MPN especially in MF.[24] We thus compared the circulating cytokine levels in PV and MF

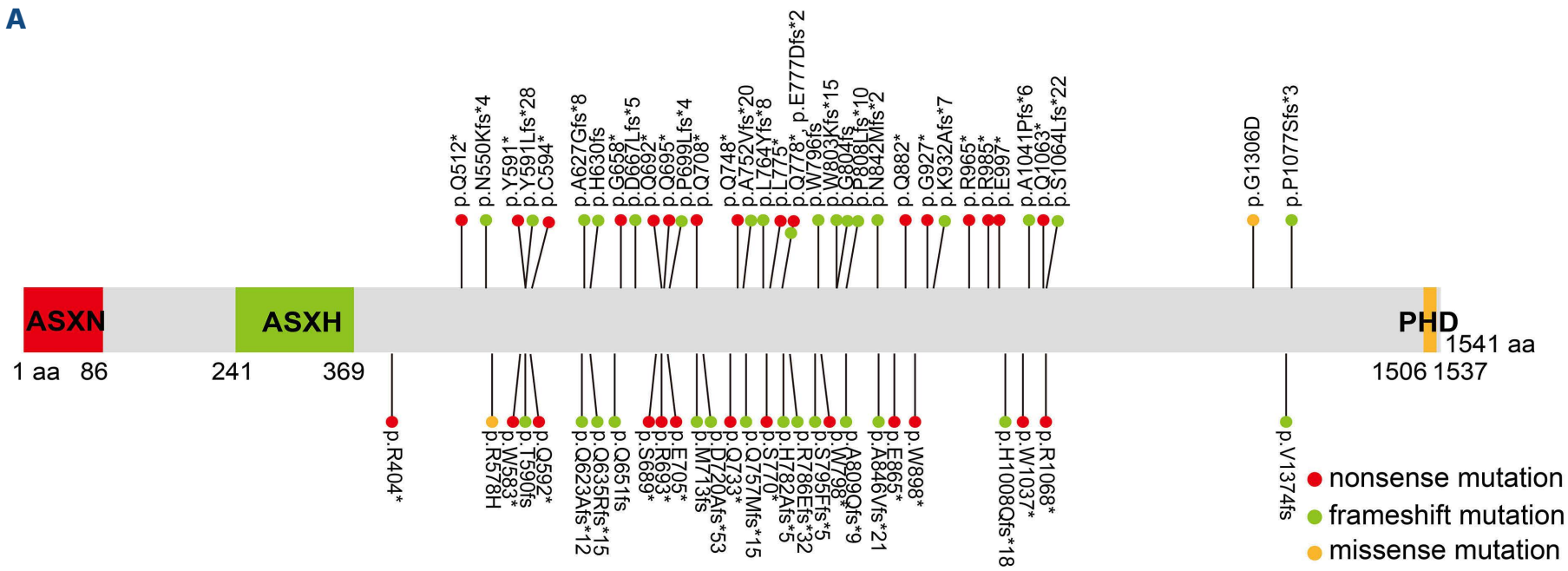

Figure 1. *ASXL1* mutations are associated with severe disease phenotypes in myelofibrosis patients. (A) Landscape of localizations and mutational types of 98 *ASXL1* mutations in 302 patients with myelofibrosis (MF). (B-D) Spleen sizes (B) (N=87 for *ASXL1*^{MT} patients and n=196 for *ASXL1*^{WT} patients), proportions of CD34^{+} cells in peripheral blood (PB) (C) (N=38 for *ASXL1*^{MT} patients and N=79 for *ASXL1*^{WT} patients), and MF grades (D) (N=98 for *ASXL1*^{MT} patients and N=204 for *ASXL1*^{WT}patients) of MF patients with different *ASXL1* mutational status. (E-G) Spleen sizes (E) (N=75 for *Driver*^{MT}*ASXL1*^{MT} patients and N=157 for *Driver*^{MT}*ASXL1*^{WT} patients), proportions of CD34^{+} cells in PB (F) (N=34 for *Driver*^{MT}*ASXL1*^{MT} patients and N=68 for *Driver*^{MT}*ASXL1*^{WT} patients) and MF grades (G) (N=85 for *Driver*^{MT}*ASXL1*^{MT} patients and N=165 for *Driver*^{MT}*ASXL1*^{WT} patients) of *driver*^{MT} MF patients with different *ASXL1* mutational status. ASXN: additional sex combs N-terminus domain; ASXH: additional sex combs homology domain; PHD: plant homeodomain. LCM: left costal margin. In (B), (C), (E) and (F), the results are presented as the median ± interquartile range. A Mann-Whitney U test was performed between the medians of two groups. In (D) and (G), the results are presented as percentages. A Mann-Whitney U test was performed between ordinal variables. *P<0.05, **P<0.01, ***P<0.001, ****P<0.0001.

patients and observed that MF patients had a more severe inflammatory environment than PV patients (*Online Supplementary Figure S5A*, *Online Supplementary Table S3*). Notably, *ASXL1*^{MT} MF patients showed higher levels of tumor necrosis factor (TNF)-α and IL-10 than *ASXL1*^{WT} MF patients (*Online Supplementary Figure S5A*, *Online Supplementary Table S3*). Moreover, a set of inflammatory cytokines and chemokines, including TNF-α, CCL2 and CCL5 were elevated in *Asxl1*$^{-/-}$*Jak2*^{VF} mice compared with *Jak2*^{VF} mice (*Online Supplementary Figure S5B*). Several cell populations, such as monocytes, granulocytes and megakaryocytes, are responsible for overproduction of cytokines in MF.[25] Remarkably, we observed that both *ASXL1*^{MT} MF patients and *Asxl1*$^{-/-}$*Jak2*^{VF} mice had elevated monocyte counts in PB (Figure 2A, *Online Supplementary Tables S1* and *2*), which are the major cell origin of cytokines in MF.[26,27] Subsequent subtype assays of PB monocytes (CD115^{+}CD11b^{+}) in mouse models revealed elev-

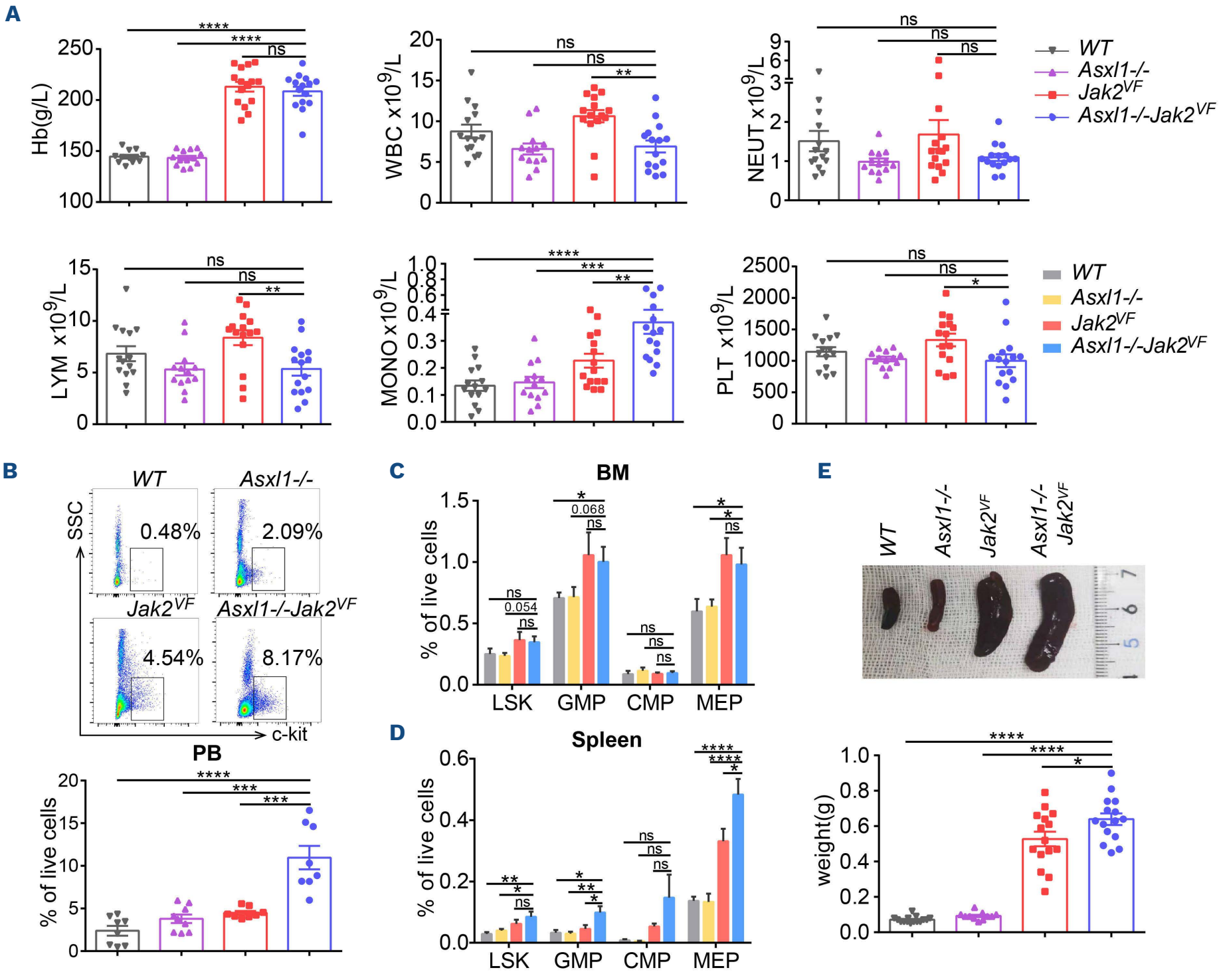

Figure 2. *Asxl1* deletion is associated with enhanced extramedullary hematopoiesis in *Asxl1*$^{-/-}$*Jak2*^{VF} mice. (A) Hemoglobin, white blood cell, neutrophil, lymphocyte, monocyte, and platelet counts in peripheral blood (PB) were assessed at 12 weeks of age in *Asxl1*$^{-/-}$*Jak2*^{VF}, *Jak2*^{VF}, *Asxl1*$^{-/-}$ and WT mice (N=13–15 per group). (B) Representative flow cytometric plots (upper) and the proportions (lower) of c-kit^{+} cells in PB of *Asxl1*$^{-/-}$*Jak2*^{VF}, *Jak2*^{VF}, *Asxl1*$^{-/-}$ and WT mice at 14-16 weeks of age (N=8–9 per group). (C, D) The proportions of LSK cells (Lin^{-}Sca-1^{+}c-kit^{+}), granulocyte/macrophage progenitors (Lin^{-}Sca-1^{-}c-kit^{+}CD34^{+}FcγRII/III^{high}), common myeloid progenitors (Lin^{-}Sca-1^{-}c-kit^{+}CD34^{+}FcγRII/III^{low}) and megakaryocyte-erythroid progenitors (Lin^{-}Sca-1^{-}c-kit^{+}CD34^{-}FcγRII/III^{-}) in bone marrow (C) and spleens (D) from *Asxl1*$^{-/-}$*Jak2*^{VF}, *Jak2*^{VF}, *Asxl1*$^{-/-}$ and WT mice at 14-16 weeks of age (N=8-9 per group). (E) Representative images (upper) and the weights (lower) of spleens from *Asxl1*$^{-/-}$*Jak2*^{VF}, *Jak2*^{VF}, *Asxl1*$^{-/-}$ and WT mice at 14-16 weeks of age (N=11-15 per group). In (A–E), the results are presented as mean ± standard error of the mean. A two-tailed unpaired Student *t* test was performed between means of two groups. ns, not significant, **P*<0.05, ***P*<0.01, ****P*<0.001, *****P*<0.0001. Hb: hemoglobin; WBC: white blood cells; NEUT: neutrophils; LYM: lymphocytes; MONO: monocytes; PLT: platelets; GMP: granulocyte/macrophage progenitors; CMP: common myeloid progenitors; MEP: megakyocyte-erythroid progenitors; SSC: side scatter; BM: bone marrow.

ated Ly6C$^+$ monocytes (inflammatory monocytes),[28] but not Ly6C$^-$ monocytes in *Asxl1$^{-/-}$Jak2^{VF}* mice (*Online Supplementary Figure S5C*). In addition, monocyte-derived dendritic cells, which accumulate during inflammatory conditions,[29] were increased in the PB of *Asxl1$^{-/-}$Jak2^{VF}* mice (Figure 4A, *Online Supplementary Figure S5D*). Consistent with PB findings, *Asxl1$^{-/-}$Jak2^{VF}* mice showed higher proportions of monocytes (CD11b$^+$CD115$^+$) in BM and spleens compared with *Jak2^{VF}* mice (Figure 4B, C, *Online Supplementary Figure S6A*), while no difference was found in granulocytes (CD11b$^+$CD115$^-$) (*Online Supplementary Figure 6B*).

Monocyte-derived macrophages are also critical in chronic inflammation. They are highly heterogeneous cells that can rapidly polarize to M1 (pro-inflammatory) or M2 (anti-inflammatory) macrophages in response to microenvironmental signals.[30] We next analyzed macrophage populations and M1/M2 polarization in mouse models. Gr-1$^-$CD115^{int}F4/80$^+$SSC^{low} cells were defined as macrophages in flow cytometry analysis and further classified as M1 (CD80$^+$CD206$^-$) and M2 (CD80$^-$CD206$^+$) subtypes.[31] The proportions of macrophages, predominantly M1 macrophages, were markedly increased in BM and spleens of *Asxl1$^{-/-}$Jak2^{VF}* mice compared with the proportions in *Jak2^{VF}* mice (Figure 4D, E; *Online Supplementary Figure S6C*). Similarly, using immunostaining, we observed that *ASXL1^{MT}* MF patients had higher numbers of CD45$^+$CD68$^+$ cells, which are composed of monocytes and macrophages, in BM specimens than those in *ASXL1^{WT}* MF patients (*Online Supplementary Figure S7, Online Supplementary Table S4*).

To confirm the origins of macrophages in mouse models, we performed genotyping identification in sorted *Asxl1$^{-/-}$Jak2^{VF}* BM macrophages and detected both the *Jak2^{V617F}* mutation and the *Asxl1* deletion (*Online Supplementary Figure S6D, E*). We next did a noncompetitive bone marrow transplantation assay (*Asxl1$^{-/-}$Jak2^{VF}* BM nucleated cells [CD45.2] to lethally irradiated recipients [CD45.1]) and measured the percentages of donor (CD45.2) and recipient (CD45.1) cells in macrophages. Nearly 90% of the total and M1 macrophages were positive for CD45.2 in BM and spleens of *Asxl1$^{-/-}$Jak2^{VF}* recipients (*Online Supplementary*

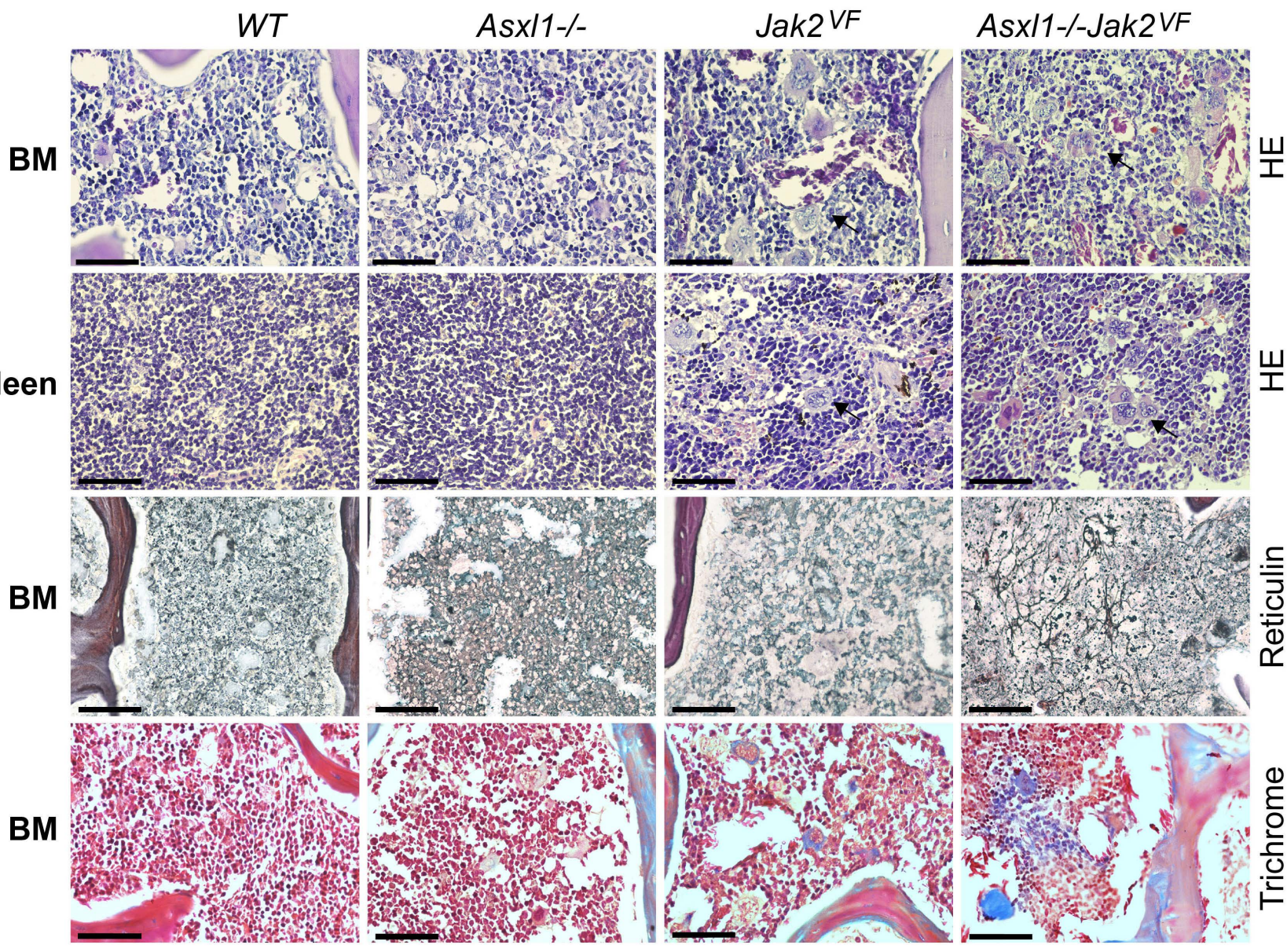

Figure 3. Morphology of enhanced extramedullary hematopoiesis and myelofibrosis in *Asxl1$^{-/-}$Jak2^{VF}* mice. Representative images of hematoxylin and eosin (H&E), Reticulin and Masson trichrome staining in femur and representative images of H&E staining in spleen biopsy specimens from *Asxl1$^{-/-}$Jak2^{VF}*, *Jak2^{VF}*, *Asxl1$^{-/-}$* and WT mice at 16 weeks of age. *Asxl1$^{-/-}$Jak2^{VF}* and *Jak2^{VF}* mice showed increased megakaryocytes and atypia in bone marrow and spleen specimens (arrow). Original magnification 40×, scale bar, 50 μm. BM: bone marrow.

Figure S6F). These data suggest that the increased macrophages are neoplastic macrophages derived from monocytes rather than primary tissue-resident macrophages. On the basis of the above findings, we questioned whether *Asxl1* deletion would lead to the differentiation bias of *Asxl1*$^{-/-}$*Jak2*^{VF} HSPC toward the monocyte/macrophage lineage. To examine this, we isolated *Asxl1*$^{-/-}$*Jak2*^{VF} and *Jak2*^{VF} BM c-kit^{+} cells and seeded them in methylcellulose

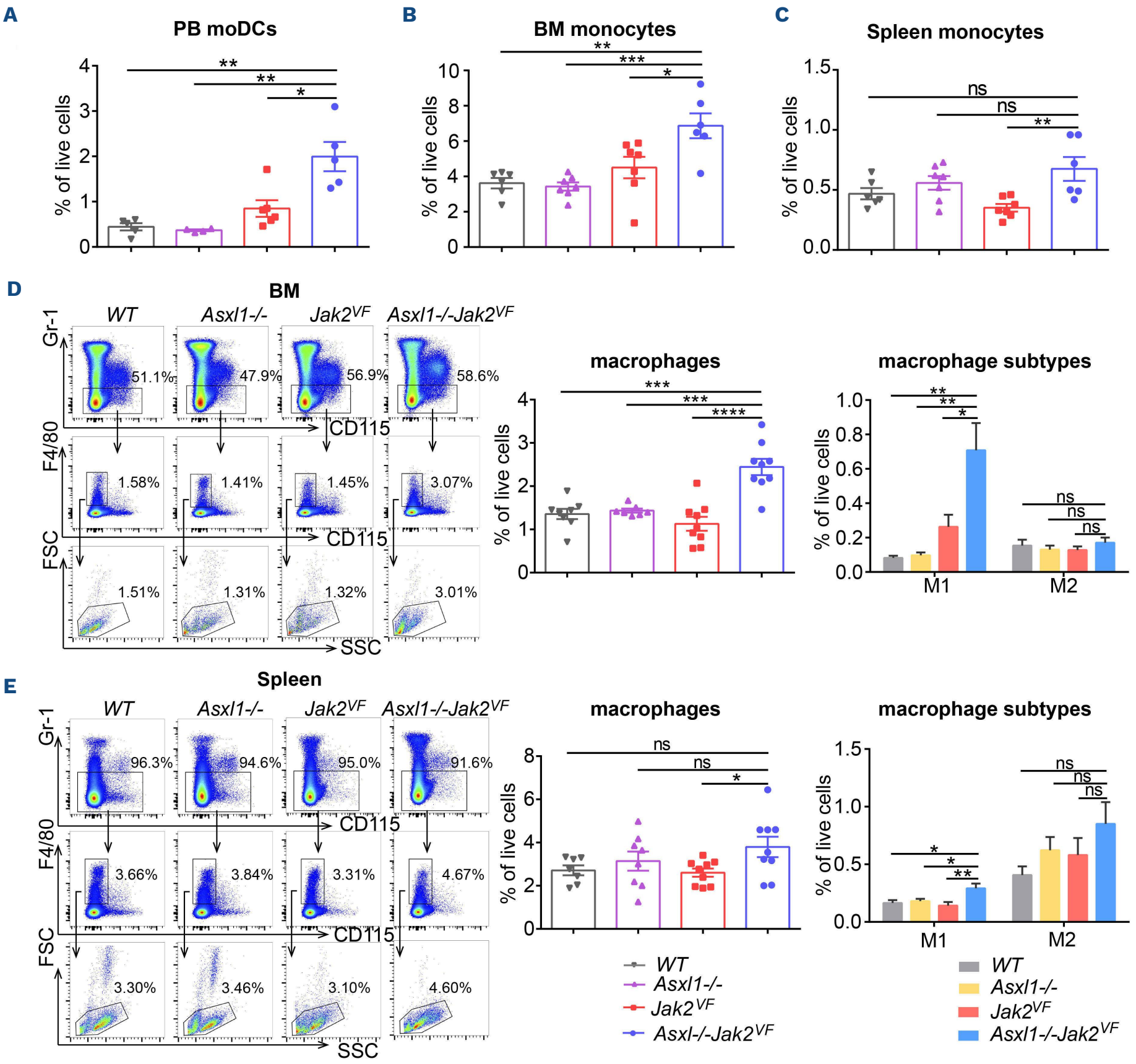

Figure 4. *ASXL1*^{MT} myelofibrosis patients and *Asxl1*$^{-/-}$*Jak2*^{VF} mice have increased inflammatory monocytes/macrophages. (A) The proportions of monocyte-derived dendritic cells (CD11c^{int}CD11b^{high}MHC II^{+}Ly6C^{+}) in peripheral blood of *Asxl1*$^{-/-}$*Jak2*^{VF}, *Jak2*^{VF}, *Asxl1*$^{-/-}$ and WT mice at 14-16 weeks of age (N=4-6 per group). (B, C) The proportions of monocytes (CD11b^{+}CD115^{+}) in bone marrow (B) and spleens (C) of *Asxl1*$^{-/-}$*Jak2*^{VF}, *Jak2*^{VF}, *Asxl1*$^{-/-}$ and WT mice at 14-16 weeks of age (N=6-7 per group). (D) Representative flow cytometric plots (left) and the proportions of total macrophages (Gr-1^{-}CD115^{int}F4/80^{+}SSC^{low}) (middle) and M1(CD80^{+}CD206^{-})/M2 (CD80^{-}CD206^{+}) subtypes (right) in bone marrow of *Asxl1*$^{-/-}$*Jak2*^{VF}, *Jak2*^{VF}, *Asxl1*$^{-/-}$ and WT mice at 14-16 weeks of age (N=7-9 per group). (E) Representative flow cytometric plots (left) and the proportions of total macrophages (Gr-1^{-}CD115^{int}F4/80^{+}SSC^{low}) (middle) and M1(CD80^{+}CD206^{-})/M2 (CD80^{-}CD206^{+}) subtypes (right) in spleens of *Asxl1*$^{-/-}$*Jak2*^{VF}, *Jak2*^{VF}, *Asxl1*$^{-/-}$ and WT mice at 14-16 weeks of age (N=7-9 per group). In (A–E), the results are presented as mean ± standard error of mean. A two-tailed unpaired Student *t* test was performed between means of two groups. ns: not significant, **P*<0.05, ***P*<0.01, ****P*<0.001, *****P*<0.0001. PB: peripheral blood; moDC: monocyte-derived dendritic cells; BM: bone marrow; SSC: side scatter; FSC: forward scatter.

supplemented with mouse IL-3 (10 ng/mL) *in vitro*. On day 8, no difference was found in the numbers of colonies between these two groups (*Online Supplementary Figure S8A*), while flow cytometric and morphological analysis of cells obtained from colonies showed higher proportions of macrophages (F4/80$^+$) in *Asxl1*$^{-/-}$*Jak2*^{VF} mice than in *Jak2*^{VF} mice (*Online Supplementary Figure S8B, C*), indicating a skewed monocyte/macrophage differentiation of *Asxl1*$^{-/-}$*Jak2*^{VF} HSPC.

Altogether, these data indicate that, in the context of a constitutively activated JAK/STAT pathway, *ASXL1* mutations induce an inflammatory monocyte/macrophage differentiation bias and enhance inflammation in *ASXL1*^{MT} MF.

ASXL1 mutations result in increased monocyte-derived fibrocyte differentiation in *ASXL1*^{MT} myelofibrosis patients and *Asxl1*$^{-/-}$*Jak2*^{VF} mice

Mesenchymal stromal cell (MSC)-derived myofibroblasts were previously considered as the major collagen-producing cells in MPN.[32-34] We performed Gli1, Leptin Receptor (LeptinR), and α-SMA immunostaining in MF patients and chose blood vessel as a positive control (*Online Supplementary Figure S9A*). However, no difference was found in MSC-derived myofibroblasts (Gli1$^+$ and/or LeptinR$^+$ and α-SMA$^+$) as well as Gli1$^+$ cells and LeptinR$^+$ cells between *ASXL1*^{WT} and *ASXL1*^{MT} MF patients (*Online Supplementary Figures S9B-D* and *S10, Online Supplementary Table S4*). Recently, several studies identified neoplastic monocyte-derived fibrocytes as a separate contributor to BM fibrosis.[22,23] Considering the increased monocytes in both *ASXL1*^{MT} MF patients and *Asxl1*$^{-/-}$*Jak2*^{VF} mice, we sought to determine whether monocyte-derived fibrocytes play a critical role in BM fibrosis formation. Monocyte-derived fibrocytes are positive for both hematopoietic markers and collagen markers.[22,23] Accordingly, we performed CD45 and ProCollagenI (ProCol-I) immunostaining of BM specimens from MF patients and observed increased fibrocytes (CD45$^+$ProCol-I$^+$) in *ASXL1*^{MT} MF patients compared with *ASXL1*^{WT} MF patients (Figure 5A, B; *Online Supplementary Table S4*).

We next isolated BM nucleated cells from *Asxl1*$^{-/-}$*Jak2*^{VF}, *Jak2*^{VF}, *Asxl1*$^{-/-}$ and WT mice and cultured them in conditions that promote the differentiation of monocytes to fibrocytes.[22,23] On day 5, the numbers of long spindle-shaped CD45$^+$CollagenI (Col-I)$^+$ fibrocytes derived from *Asxl1*$^{-/-}$*Jak2*^{VF} BM nucleated cells were higher than those derived from cells of other genotypes (Figure 5C, D). Genotyping detected the *Jak2*^{V617F} mutation and *Asxl1* deletion in cultured fibrocytes, confirming that the fibrocytes were originated from malignant clones (*Online Supplementary Figure S11A–B*). We also measured the proportions of fibrocytes (CD45$^+$Col-I$^+$, CD11b$^+$Col-I$^+$ or CD68$^+$Col-I$^+$) using flow cytometry and observed that *Asxl1*$^{-/-}$*Jak2*^{VF} mice exhibited markedly increased fibrocytes in both BM and spleens compared with other genotypes (Figure 5E, F; *Online Supplementary Figure S11C–D*).

Overall, these results establish that increased neoplastic monocyte-derived fibrocytes may be associated with acceleration of BM fibrosis in *ASXL1*^{MT} MF patients and *Asxl1*$^{-/-}$*Jak2*^{VF} mice.

Asxl1 deletion results in derepression of polycomb group target genes in *Asxl1*$^{-/-}$*Jak2*^{VF} mice

ASXL1 deletion impairs hematopoiesis and accelerates myeloid malignancies via aberrant histone modifications and dysregulated transcription.[35] We thus performed bulk RNA sequencing, ATAC sequencing and ChIP sequencing on *Asxl1*$^{-/-}$*Jak2*^{VF} and *Jak2*^{VF} BM c-kit$^+$ cells to elucidate the transcriptional and associated epigenetic alterations after *Asxl1* deletion. The expression profiles of *Asxl1*$^{-/-}$*Jak2*^{VF} BM c-kit$^+$ cells showed distinct clusters from *Jak2*^{VF} cells in principal component analysis (Figure 6A). As shown by the heatmap, 2,352 genes were significantly upregulated and 1,504 genes significantly downregulated in *Asxl1*$^{-/-}$*Jak2*^{VF} BM c-kit$^+$ cells compared with *Jak2*^{VF} cells (fold change >2, P<0.05) (Figure 6B). Interestingly, gene set enrichment analysis showed that the upregulated genes in *Asxl1*$^{-/-}$*Jak2*^{VF} were significantly associated with *bona fide* PcG target genes, as identified by the overlap between H3K27me3 and H2AK119ub1 ChIP-sequencing experiments on *Asxl1*$^{-/-}$*Jak2*^{VF} and *Jak2*^{VF} BM c-kit$^+$ cells (Figure 6C, D). This is consistent with the genetic categorization of *ASXL1* as a PcG gene.[36] Integrated analysis of RNA-sequencing and ATAC-sequencing data showed that there was a significant increase of chromatin accessibility associated with upregulated genes (Figure 6E) and these sites with gained accessibility were enriched with increased levels of H3K4me1 and H3K27ac, histone marks of active enhancers in *Asxl1*$^{-/-}$*Jak2*^{VF} BM c-kit$^+$ cells (Figure 6E). Figure 6F shows the changes of representative PcG target genes *Jun* and *Egr1*. Taken together, these results demonstrate that *Asxl1* deletion results in the derepression of PcG target genes by activating their enhancers in *Asxl1*$^{-/-}$*Jak2*^{VF} BM c-kit$^+$ cells.

Activated EGR1-TNFA axis enhances monocyte/macrophage and fibrocyte differentiation in *ASXL1*^{MT} myelofibrosis patients and *Asxl1*$^{-/-}$*Jak2*^{VF} mice

To explore the critical driving genes for disease phenotypes, we next performed bulk RNA sequencing on BM c-kit$^+$ cells of all genotypes and finally focused on 45 genes that were upregulated in *Asxl1*$^{-/-}$*Jak2*^{VF} BM c-kit$^+$ cells compared with those in the other three genotypes (Figure 7A). Analysis of Kyoto Encyclopedia of Genes and Genomes (KEGG) pathways revealed the enrichment of several inflammation-related pathways including TNF, IL-17 and NF-KB pathways (Figure 7B). Notably, in line with the activated TNF pathway, TNF-α levels were elevated in serum of *ASXL1*^{MT} MF patients and *Asxl1*$^{-/-}$*Jak2*^{VF} mice (*Online Sup-*

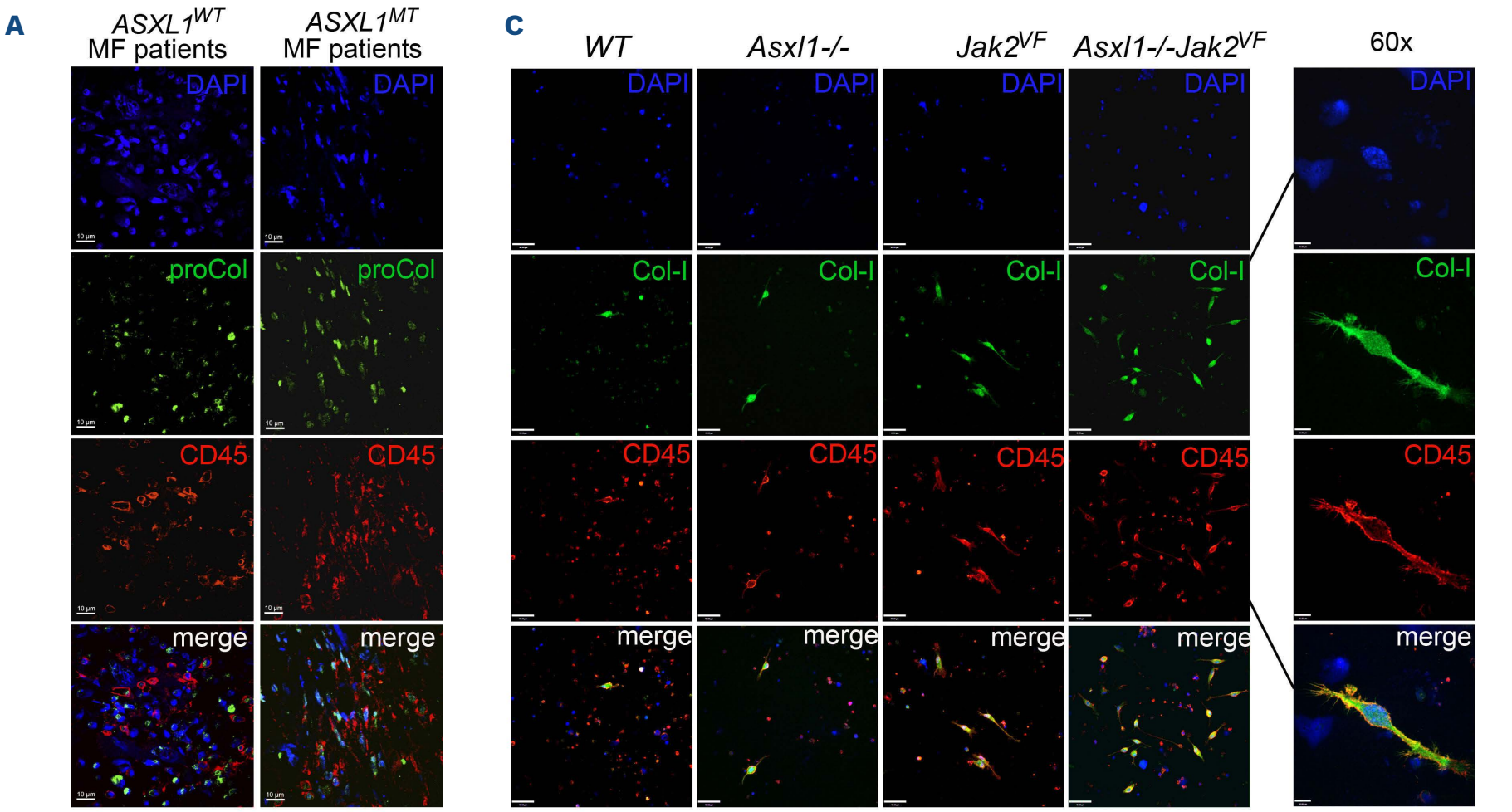

Figure 5. Increased monocyte-derived fibrocytes in both *ASXL1*^{MT} myelofibrosis patients and *Asxl1*$^{-/-}$*Jak2*^{VF} mice. (A) Representative immunofluorescence imaging of fibrocytes (ProCol-I^{+}CD45^{+}) in bone marrow (BM) specimens from patients with myelofibrosis (MF). Original magnification 60×; scale bar, 10 μm. (B) The number of fibrocytes in BM specimens of *ASXL1*^{WT} and *ASXL1*^{MT} MF patients (N=8 for *ASXL1*^{WT} patients and N=8 for *ASXL1*^{MT} patients, median= 20.5 cells/10 high power field [HPF] for *ASXL1*^{WT} patients and 74.0 cells/10 HPF for *ASXL1*^{MT} patients). (C) Representative immunofluorescence images of fibrocytes (Col-I^{+}CD45^{+}) from BM nucleated cells of 14-week-old *Asxl1*$^{-/-}$*Jak2*^{VF}, *Jak2*^{VF}, *Asxl1*$^{-/-}$ and WT mice cultured in conditions that promote differentiation to fibrocytes. Left: original magnification 20×; scale bar, 40 μm; right: original magnification 60×; scale bar, 10 μm. (D) The numbers of fibrocytes derived from *Asxl1*$^{-/-}$*Jak2*^{VF}, *Jak2*^{VF}, *Asxl1*$^{-/-}$ and WT BM nucleated cells cultured for 5 days (N=3-4 per group). (E, F) The proportions of fibrocytes in BM (E) and spleens (F) of *Asxl1*$^{-/-}$*Jak2*^{VF}, *Jak2*^{VF}, *Asxl1*$^{-/-}$ and WT mice at 14-16 weeks of age determined using flow cytometry (N=5-6 per group). In (B), the results are presented as median ± interquartile range. A Mann-Whitney U test was performed between medians of two groups. In (D-F), the results are presented as mean ± standard error of mean. A two-tailed unpaired Student *t* test was performed between means of two groups. *P<0.05, **P<0.01, ***P<0.001, ****P<0.0001.

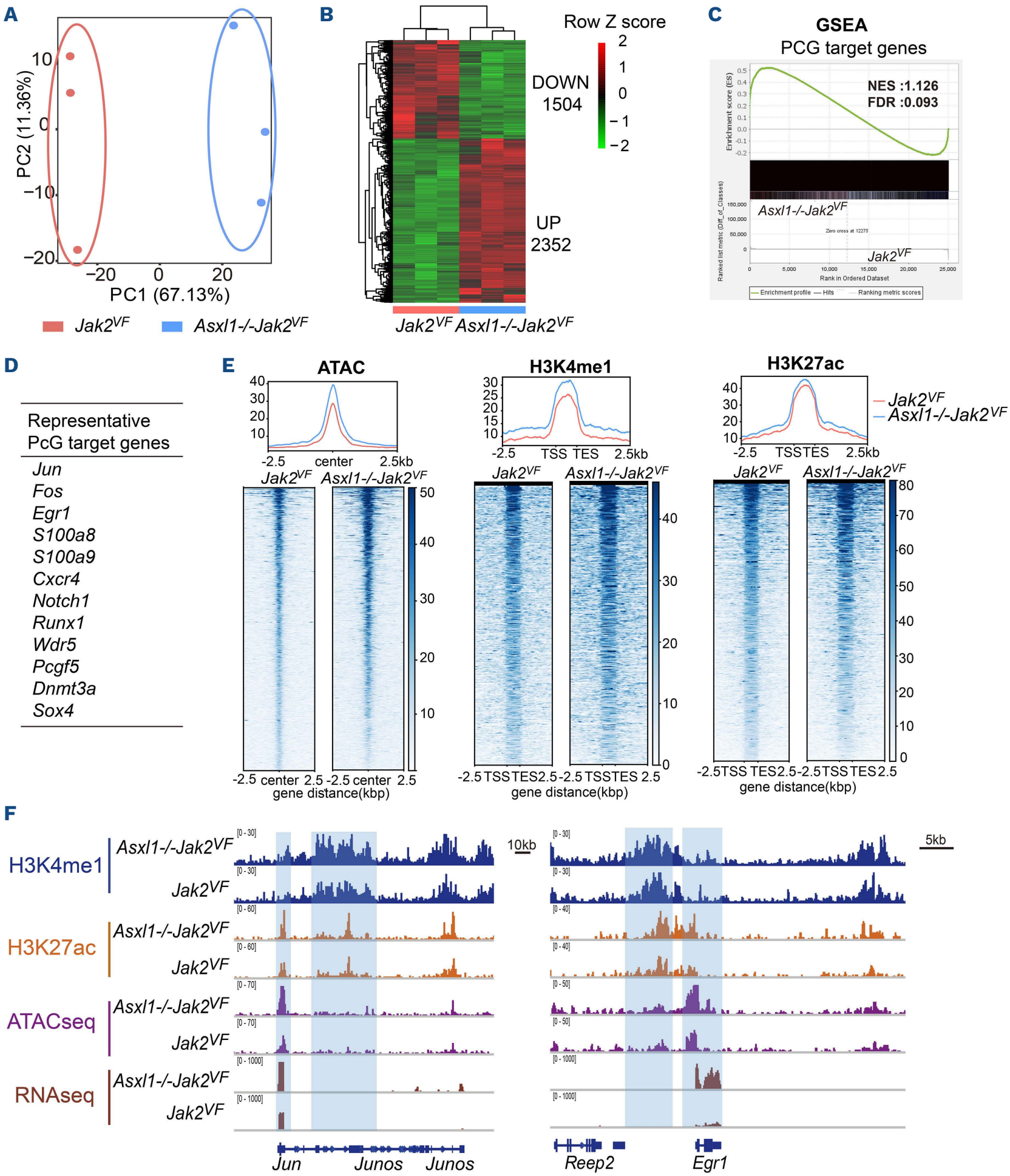

Figure 6. *Asxl1* deletion results in derepression of polycomb group target genes in *Asxl1*$^{-/-}$*Jak2*^{VF} bone marrow c-kit^{+} cells. (A) Principal component analysis plot showing the gene-expression profile of bone marrow (BM) c-kit^{+} cells from *Asxl1*$^{-/-}$*Jak2*^{VF} and *Jak2*^{VF} mice. Each dot represents an independent biological sample. (B) Heatmap showing significantly upregulated and downregulated genes in *Asxl1*$^{-/-}$*Jak2*^{VF} BM c-kit^{+} cells compared with *Jak2*^{VF} BM c-kit^{+} cells (fold change >2, P<0.05). (C) Gene set enrichment analysis (GSEA) showed that polycomb group (PcG) target genes were significantly depressed in *Asxl1*$^{-/-}$*Jak2*^{VF} BM c-kit^{+} cells when compared to *Jak2*^{VF} BM c-kit^{+} cells. PcG target genes were defined by the 4,700 regions co-occupied by H3K27me3 and H2AK119ub1 from ChIP-sequencing data of *Asxl1*$^{-/-}$*Jak2*^{VF} and *Jak2*^{VF} BM c-kit^{+} cells. (D) Representative enriched PcG target genes in *Asxl1*$^{-/-}$*Jak2*^{VF} BM c-kit^{+} cells in GSEA. (E) Metaplots and heatmaps of ATAC sequencing, and H3K4me1 and H3K27ac ChIP sequencing at upregulated genes in *Asxl1*$^{-/-}$*Jak2*^{VF} BM c-kit^{+} cells and *Jak2*^{VF} BM c-kit^{+} cells. (F) Snapshot of the genomic view for H3K4me1 and H3K27ac ChIP sequencing, ATAC sequencing and RNA sequencing at the representative PcG target gene *Jun* and *Egr1* loci. ATAC: assay for transposase-accessible chromatin; Chip: chromatin immunoprecipitation.

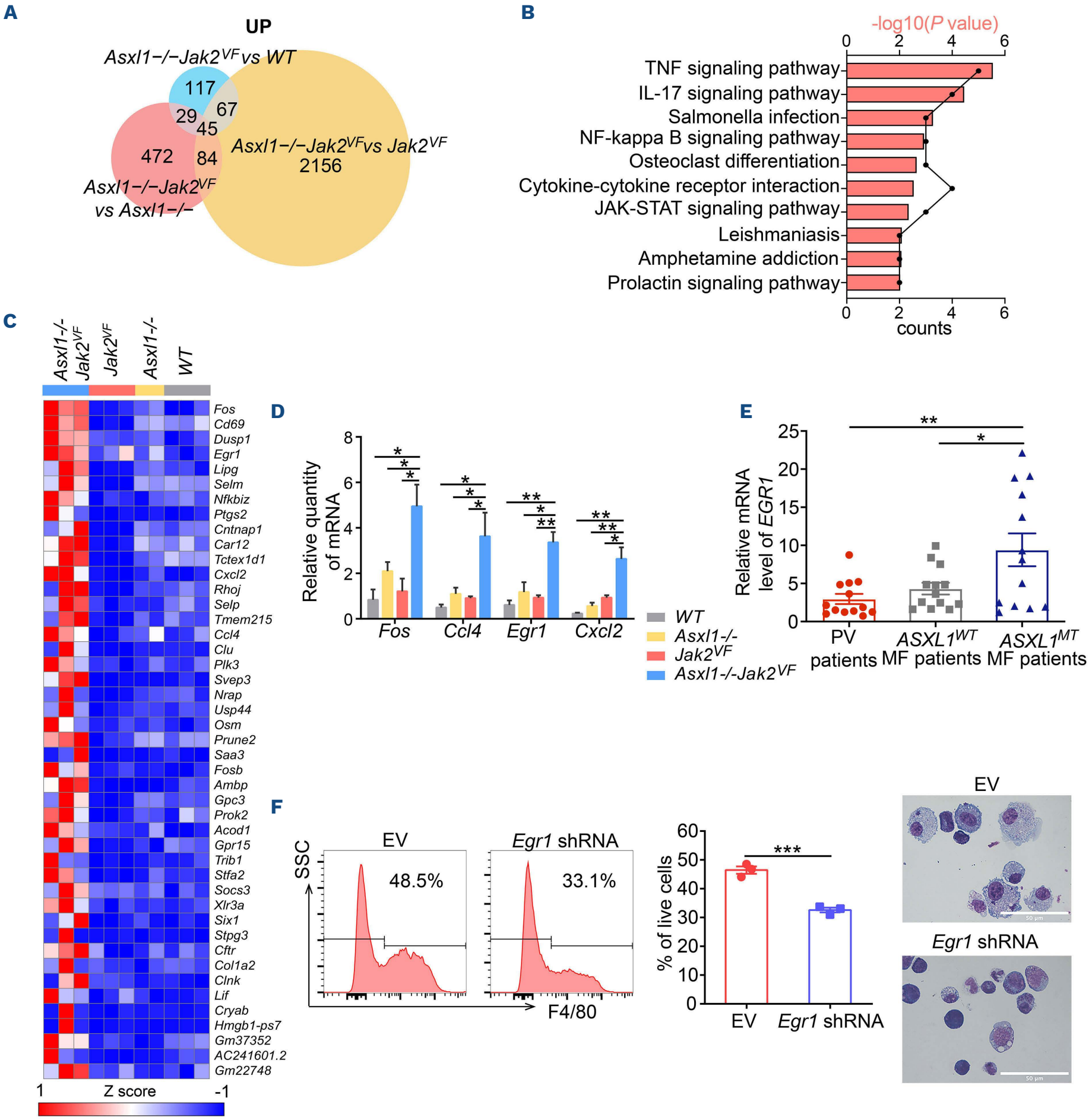

Figure 7. Activated EGR1 enhances monocyte/macrophage differentiation in *Asxl1*$^{-/-}$*Jak2*^{VF} mice. (A-C) Venn diagram (A), KEGG pathway enrichment analysis (B), and heatmap (C) of upregulated genes in *Asxl1*$^{-/-}$*Jak2*^{VF} compared with *Jak2*^{VF}, *Asxl1*$^{-/-}$ and WT BM c-kit^{+} cells (fold change >2, *P*<0.05). (D) Relative expressions of *Fos*, *Ccl4*, *Egr1* and *Cxcl2* mRNA were measured in *Asxl1*$^{-/-}$*Jak2*^{VF}, *Jak2*^{VF}, *Asxl1*$^{-/-}$ and WT bone marrow (BM) c-kit^{+} cells by real-time quantitative polymerase chain reaction (RT-qPCR) and normalized with one sample of *Jak2*^{VF} mice (N=3-4 per group). (E) Relative expressions of *EGR1* mRNA in BM mononuclear cells from polycythemia vera (PV), *ASXL1*^{MT} and *ASXL1*^{WT} myelofibrosis patients measured by RT-qPCR and normalized with one sample of PV patients (N=13 per group). (F) Representative flow cytometric plots (left) and the proportions (middle) of F4/80^{+} cells and photomicrographs of Wright-Giemsa-stained cytospin smears (right) obtained from colonies generated by *Asxl1*$^{-/-}$*Jak2*^{VF} BM c-kit^{+} cells transduced with either empty vector or *Egr1* short hairpin RNA (N=3 independent experiments). In (D-F), the results are presented as mean ± standard error of mean. A two-tailed unpaired Student *t* test was performed between means of two groups. ns, not significant, *P<0.05, **P<0.01, ***P<0.001, ****P<0.0001. MF: myelofibrosis; SSC: side scatter; EV: empty vector; shRNA: short hairpin RNA.

plementary Figure S5A, B). Several inflammation-related genes, such as *Egr1*, *Fos*, *Cxcl2* and *Ccl4*, were also upregulated in *Asxl1*$^{-/-}$*Jak2* BM c-kit^{+} cells (Figure 7C), which was validated by real-time quantitative polymerase chain reaction analysis (Figure 7D). Among *Tnfa*- and inflammation-related genes, the PcG target gene *Egr1*, was of special interest to us and validated by western blot in BM c-kit^{+} cells (*Online Supplementary Figure S12*). Upregulated *Egr1* can stimulate HSPC along the monocyte/macrophage lineage.[37] We further measured its expression in LSK cells, granulocyte/macrophage progenitors and monocytes, and detected comparable upregulation in different cell populations in *Asxl1*$^{-/-}$*Jak2*^{VF} and *Jak2*^{VF} mice (*Online Supplementary Figure S13*), which was reminiscent of monocyte/macrophage bias in *Asxl1*$^{-/-}$*Jak2*^{VF} mice and *ASXL1*^{MT} MF patients. We confirmed the upregulated *EGR1* expression in BM mononuclear cells of *ASXL1*^{MT} MF patients compared with PV and *ASXL1*^{WT} MF patients (Figure 7E, *Online Supplementary Table S5*). Increased chromatin accessibility and enhancer activation were consistently observed at the *Egr1* locus in *Asxl1*$^{-/-}$*Jak2*^{VF} BM c-kit^{+} cells (Figure 6F).

We then assessed the causal effect of *Egr1* on monocyte/macrophage differentiation. After being transduced with lentivirus-expressing control (empty vector) or specific short hairpin RNA (shRNA) against *Egr1*, *Asxl1*$^{-/-}$*Jak2*^{VF} BM c-kit^{+} cells were sorted for expression of green fluorescence protein (GFP) and seeded in methylcellulose supplemented with mouse IL-3 (10 ng/mL) *in vitro*. On day 8, we observed that *Egr1* knockdown significantly reduced the percentage of macrophages (F4/80^{+}) derived from *Asxl1*$^{-/-}$*Jak2*^{VF} BM c-kit^{+} cells (Figure 7F).

Apart from participating in hematopoietic differentiation, EGR1 also acts as a master transcription factor to activate *TNFA* expression. Luciferase activity assay and electrophoretic mobility shift assay have detected the EGR1 binding site on the TNFA promoter in human monocytic cells.[38] We next measured the expression of *Tnfa* mRNA in *Asxl1*$^{-/-}$*Jak2*^{VF} BM c-kit^{+} cells transduced with empty vector or shRNA against *Egr1*. As shown in Figure 8A, *Tnfa* expression failed to be upregulated after knockdown of *Egr1*, and TNF-α production was reduced after knockdown of Egr1 in BM c-kit^{+} cells as well (*Online Supplementary Figure S14*). In MPN, TNF-α facilitates the expansion of *JAK2*^{V617F}-positive clones,[39] and its activation was also recently identified as an early event in fibrosis-driving MSC.[40] We thus speculated that TNF-α might promote the differentiation of fibrocytes in *Asxl1*$^{-/-}$*Jak2*^{VF} mice. *In vitro* experiments showed that the numbers of cultured fibrocytes derived from BM nucleated cells treated with murine TNF-α (2 ng/mL) were significantly higher than those of cells treated with dimethyl sulfoxide, and the addition of the TNF-α receptor (TNFR) antagonist R-7050 (1 μM) eliminated this effect (Figure 8B). Moreover, R-7050 (1 μM) alone could also decrease the production of fibrocytes (Figure 8B). We also examined the effect of TNF-α on fibrocyte differentiation in the other three genotypes and observed that TNF-α promoted fibrocyte differentiation regardless

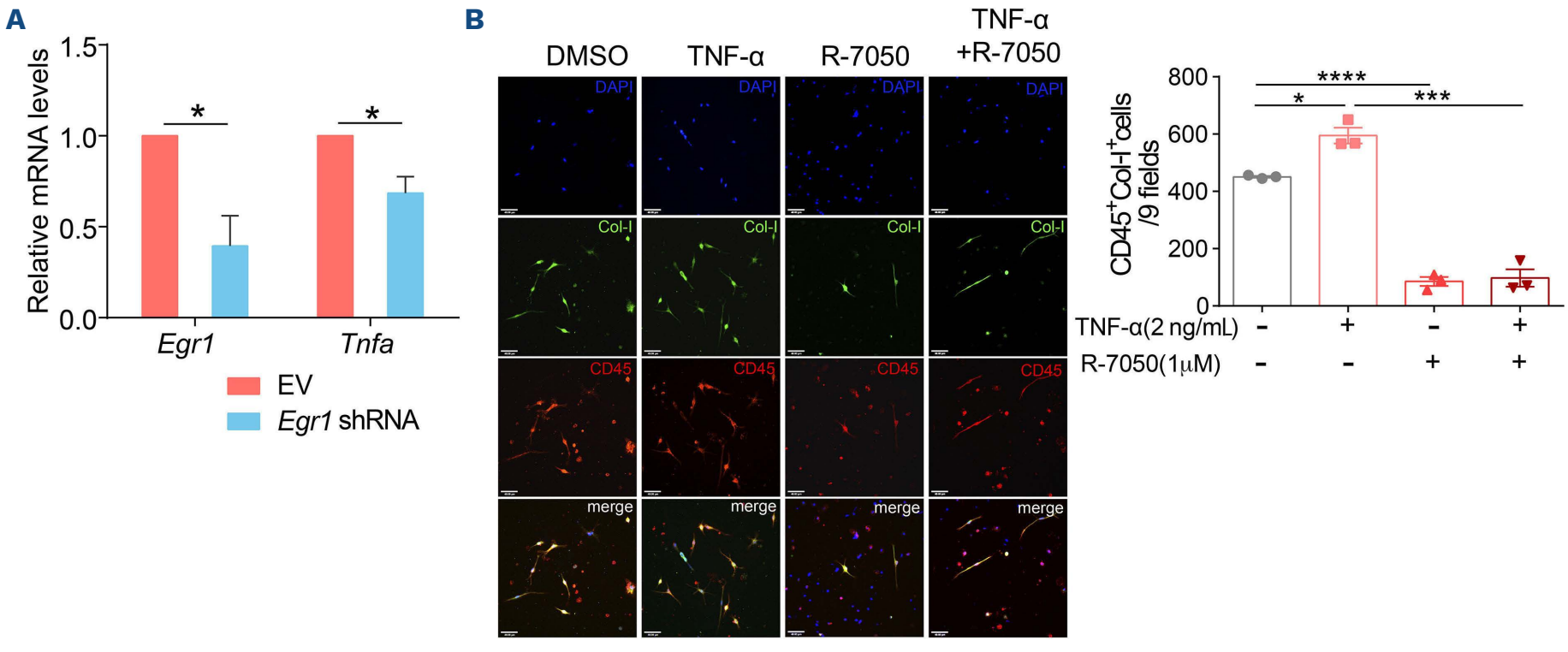

Figure 8. TNF-α promotes monocyte-derived fibrocyte differentiation in *Asxl1*$^{-/-}$*Jak2*^{VF} mice. (A) Relative expressions of *Egr1* and *Tnfa* mRNA in *Asxl1*$^{-/-}$*Jak2*^{VF} bone marrow (BM) c-kit^{+} cells infected with either empty vector or *Egr1* shRNA (3 independent experiments). (B) Representative immunofluorescence imaging (left) and numbers (right) of cultured fibrocytes derived from *Asxl1*$^{-/-}$*Jak2*^{VF} BM nucleated cells treated with dimethyl sulfoxide, mouse TNF-α (2 ng/mL), the TNF-α receptor antagonist, R-7050 (1 μM), and mouse TNF-α (2 ng/mL) combined with R-7050 (1 μM) (N=3 per group). Original magnification 20× for images; scale bar, 40 μm. The results are presented as mean ± standard error of mean. A two-tailed unpaired Student *t* test was performed between means of two groups. *P<0.05, ***P<0.001, ****P<0.0001. EV: empty vector; DMSO: dimethyl sulfoxide; TNF-α: tumor necrosis factor-alpha. shRNA: short hairpin RNA.

of *Asxl1* and *Jak2* mutational status (*Online Supplementary Figure S15A-C*). To further validate the effect of *Egr1* on fibrocyte production in *Asxl1*$^{-/-}$*Jak2*^{VF} mice, we also transfected *Asxl1*$^{-/-}$*Jak2*^{VF} BM nucleated cells with *Egr1* shRNA or an empty vector and performed an *in vitro* fibrocyte differentiation assay. As shown in *Online Supplementary Figure S16*, the number of fibrocytes significantly reduced after *Egr1* knockdown in *Asxl1*$^{-/-}$*Jak2*^{VF} mice, confirming the effect of *Egr1* on fibrocyte production.

Previous studies found no significant effects of ruxolitinib on fibrocyte differentiation in samples from patients with PMF.[23] We thus wondered whether combined inhibition of the JAK/STAT pathway and the TNFR antagonist would suppress fibrocyte differentiation. Excitingly, combining ruxolitinib (100 nM) with R-7050 (1 μM) enhanced the inhibitory effects on fibrocytes compared to the effects of ruxolitinib monotherapy (*Online Supplementary Figure S17A*), and the efficacy was confirmed in BM mononuclear cells from MF patients (*Online Supplementary Figure S17B*). Notably, ruxolitinib (100 nM) alone significantly reduced the number of cultured fibrocytes derived from *Asxl1*$^{-/-}$*Jak2*^{VF} BM nucleated cells while it did not reduce fibrocyte differentiation of BM mononuclear cells from MF patients (*Online Supplementary Figure S17A, B*), which was consistent with a previous study of PMF patients' samples.[23]

Collectively, our data indicate that an activated EGR1-TNFA axis is involved in monocyte-derived fibrocyte differentiation in *ASXL1*^{MT} MF and shed light on an attractive combination therapy for anti-fibrosis treatment.

Discussion

Mutated *ASXL1* is associated with severe MF-related features in MF patients. Whether *ASXL1* mutations are gain-of-function or loss-of-function remains a question in myeloid malignancies. Several studies have shown that gain-of-function of truncated *ASXL1* mutations contributes to myeloid malignancies,[41,42] while neither full-length nor truncated ASXL1 protein was found in *ASXL1*-mutated human myeloid leukemia cell lines and clinical samples.[18] In this study, we generated a different kind of mouse model for *Asxl1* knockout and J*ak2*^{V617F} MPN, using hematopoietic cell-specific expression as opposed to a prior germline study.[20] Our phenotype findings are consistent with previous results in germline *Asxl1*$^{+/-}$ and J*ak2*^{V617F} mouse models, suggesting the crucial role of *ASXL1* mutations in MPN progression. Moreover, we further explored the putative mechanism of *ASXL1* mutations in MPN progression.

An activated JAK/STAT pathway enhances inflammatory cytokine production and participates in malignant clonal expansion, BM fibrosis and osteosclerosis in MPN.[43] Monocytes are the principal source of inflammatory cytokines in MF patients.[27] Both *ASXL1*^{MT} MF patients and *Asxl1*$^{-/-}$*Jak2*^{VF} mice exhibit expansion of monocytes, especially inflammatory-related Ly6C^{+} monocytes. Ly6C^{+} monocytes further differentiate into M1 macrophages or monocyte-derived dendritic cells in response to inflammatory stimuli and these differentiated cells, in turn, secrete cytokines,[28] creating a positive feedback loop, which results in a vicious cycle of inflammatory cytokine production. Hence, these data suggest that skewed monocyte and macrophage differentiation results in enhanced inflammation in *ASXL1*^{MT} MF.

MF was thought to be a reactive phenomenon caused by the interaction between malignant hematopoiesis and the BM microenvironment, mediated by profibrotic cytokines.[34,44] Some studies found that Gli1^{+} and LeptinR^{+} WT MSC were functionally reprogrammed and differentiated into myofibroblasts and contributed to MF.[32,33,40] In our cohort, no difference was found in MSC-derived myofibroblasts between *ASXL1*^{MT} and *ASXL1*^{WT} MF patients, suggesting that other fibrosis-driving cells may be the major contributors to the acceleration of fibrosis in *ASXL1*^{MT} MF. Fibrocytes are derived from monocytes and initially identified in tissue fibrosis diseases such as end-stage liver or kidney diseases.[45,46] Neoplastic fibrocytes were first found in PMF patients by Verstovsek *et al.*[23] and recently reported to be present in J*ak2*^{V617F} mouse models as well.[22] Deletion or inhibition of neoplastic fibrocytes can ameliorate MPN phenotypes in MPN mouse models, suggesting their crucial role in fibrosis formation.[22,23] Using mouse models and patients' samples, our results suggest that *ASXL1* mutations accelerate BM fibrosis by reprograming the fibrosis-driving potential of hematopoietic cells to fibrocytes, and further confirm that neoplastic fibrocytes are the major contributors to BM fibrosis.

The deregulated cells identified upon *Asxl1* deletion and the derepression of PcG target genes support the concept that *ASXL1* acts as a PcG gene. Mechanistically, we demonstrated that *Asxl1* deletion results in increased chromatin accessibility and enhancer activation at derepressed genes. Nevertheless, it still remains elusive why ASXL1 biochemically antagonizes PRC1 catalytic activity while genetically acting as a transcription repressor. Two recent studies in embryonic stem cell models showed that Bap1 loss results in pervasive accumulation of H2AK119ub1 and PRC titration away from its target promoters.[47,48] Future studies will be required to test these mechanisms in the *Asxl1*$^{-/-}$ mouse model.

Notably, *Asxl1* deletion activates the enhancer at the PcG target gene *Egr1* locus and consequently upregulates *Tnfa* in *Asxl1*$^{-/-}$*Jak2*^{VF} BM c-kit^{+} cells. Activated Egr1 increases *Asxl1*$^{-/-}$*Jak2*^{VF} HSPC commitment to monocyte/macrophage lineage and stimulates TNF-α secretion. Interestingly, we detected elevated TNF-α levels uniquely in *ASXL1*^{MT} MF patients, indicating a relationship between this

cytokine and disease phenotype caused by *ASXL1* mutations. TNF-α is an essential cytokine in MPN and its absence attenuates disease phenotypes in *Jak2*^{V617F} mice through limiting the expansion of clones.[26,39] Our study indicates that TNF-α most likely enhances fibrosis by promoting differentiation of monocytes to fibrocytes, and this effect is not malignant-specific. Thus, an Egr1-mediated monocyte/macrophage differentiation bias and TNF-α secretion synergistically resulted in increased fibrocyte production and accelerated BM fibrosis in *ASXL1*^{MT} MF. Previous research and our data have confirmed that ruxolitinib has little effect on fibrocyte differentiation in MF patients' samples *in vitro*.[23] We therefore combined ruxolitinib with a TNFR antagonist and found remarkably reduced fibrocyte differentiation *in vitro*. Future *in vivo* experiments with genetic models and patient-derived xenograft models are necessary to confirm the efficacy and safety of the combination further.

In conclusion, our study illustrates the crucial role of *ASXL1* mutation in MPN phenotypes and the onset of BM fibrosis. *ASXL1* mutations activate the EGR1-TNFA axis in MPN, leading to monocyte/macrophage-mediated inflammation and neoplastic fibrocyte-induced BM fibrosis. Ruxolitinib together with a TNFR antagonist may mitigate fibrocyte production, providing an attractive theoretical approach to anti-fibrosis treatment.

Disclosures

No conflicts of interest to disclose.

Contributions

ZJX, XDW, BL, GH and ZXS conceived the idea of this study; ZXS, JQL,YYZ, BL, XDW, HG and ZJX designed the research; ZXS, JQL, YYZ, LY, YNC, PHZ, WJZ, YRY and HJH performed research; JYW, XY, TJQ, ZFX, LJP and SQQ collected clinical data; ZXS, JQL, YYZ and YNC analyzed data; ZXS, JQL, YYZ, ZXL and YNC performed statistical and bioinformatic analyses; ZXS, YYZ, BL, XDW, GH and ZJX wrote the manuscript; and all authors reviewed and approved the manuscript. The authorship order among co-first authors was assigned according to working hours and contributions.

Acknowledgments

The authors would like to thank Bin Li (State Key Laboratory of Experimental Hematology) and Ningpu Ban (Pathology Center, Blood Diseases Hospital, CAMS) for assistance in preparation of murine pathology sections. We thank the State Key Laboratory of Experimental Hematology Flow Cytometry Center, Experimental Animal Center and Image Center for assistance with the experiments.

Funding

This study was supported in part by National Natural Science funds (N. 81530008, 81870104 and 82170139 to ZJX, 82070134 and 81600098 to BL, 81770129 to GH, and 81772676 and 31970579 to XDW), the National Key Research and Development Program (N. 2017YFA0504102 to XDW), Tianjin Natural Science funds (N. 18JCZDJC34900 to ZJX, 18JCJQJC48200 to XDW, and 19JCQNJC09400 to BL), the PUMC Youth Fund and Fundamental Research Funds for Central Universities (N. 3332019093 to JQL), CAMS Initiative Fund for Medical Sciences (N. 2016-I2M-1-001 and 2020-I2M-C&T-A-020 to ZJX, and 2020-I2M-C&T-B-090 to ZFX), and the Haihe Laboratory of Cell Ecosystem Innovation Fund (N. HH22KYZX0033 to ZJX).

Data-sharing statement

The murine RNA-sequencing, ATAC-sequencing and ChIP-sequencing data reported in this paper are available at the NCBI's Gene Expression Omnibus (GEO) under accession number: GSE181291.

References

1. Nangalia J, Green AR. Myeloproliferative neoplasms: from origins to outcomes. Blood. 2017;130(23):2475-2483.
2. Tefferi A. Primary myelofibrosis: 2021 update on diagnosis, risk-stratification and management. Am J Hematol. 2021;96(1):145-162.
3. James C, Ugo V, Le Couédic JP, et al. A unique clonal JAK2 mutation leading to constitutive signalling causes polycythaemia vera. Nature. 2005;434(7037):1144-1148.
4. Pikman Y, Lee BH, Mercher T, et al. MPLW515L is a novel somatic activating mutation in myelofibrosis with myeloid metaplasia. PLoS Med. 2006;3(7):e270.
5. Nangalia J, Massie CE, Baxter EJ, et al. Somatic CALR mutations in myeloproliferative neoplasms with nonmutated JAK2. N Engl J Med. 2013;369(25):2391-2405.
6. Tefferi A. Challenges facing JAK inhibitor therapy for myeloproliferative neoplasms. N Engl J Med. 2012;366(9):844-846.
7. Akada H, Yan D, Zou H, Fiering S, Hutchison RE, Mohi MG. Conditional expression of heterozygous or homozygous Jak2V617F from its endogenous promoter induces a polycythemia vera-like disease. Blood. 2010;115(17):3589-3597.
8. Xing S, Wanting TH, Zhao W, et al. Transgenic expression of JAK2V617F causes myeloproliferative disorders in mice. Blood. 2008;111(10):5109-5117.
9. Mullally A, Lane SW, Ball B, et al. Physiological Jak2V617F expression causes a lethal myeloproliferative neoplasm with differential effects on hematopoietic stem and progenitor cells. Cancer Cell. 2010;17(6):584-596.
10. Vannucchi AM, Lasho TL, Guglielmelli P, et al. Mutations and prognosis in primary myelofibrosis. Leukemia. 2013;27(9):1861-1869.
11. Li B, Gale RP, Xu Z, et al. Non-driver mutations in myeloproliferative neoplasm-associated myelofibrosis. J Hematol Oncol. 2017;10(1):99.
12. Yang Y, Akada H, Nath D, Hutchison RE, Mohi G. Loss of Ezh2 cooperates with Jak2V617F in the development of myelofibrosis

in a mouse model of myeloproliferative neoplasm. Blood. 2016;127(26):3410-3423.
13. Chen E, Schneider RK, Breyfogle LJ, et al. Distinct effects of concomitant Jak2V617F expression and Tet2 loss in mice promote disease progression in myeloproliferative neoplasms. Blood. 2015;125(2):327-335.
14. Jacquelin S, Straube J, Cooper L, et al. Jak2V617F and Dnmt3a loss cooperate to induce myelofibrosis through activated enhancer-driven inflammation. Blood. 2018;132(26):2707-2721.
15. Simon J, Chiang A, Bender W. Ten different Polycomb group genes are required for spatial control of the abdA and AbdB homeotic products. Development. 1992;114(2):493-505.
16. Dey A, Seshasayee D, Noubade R, et al. Loss of the tumor suppressor BAP1 causes myeloid transformation. Science. 2012;337(6101):1541-1546.
17. Wu X, Bekker-Jensen IH, Christensen J, et al. Tumor suppressor ASXL1 is essential for the activation of INK4B expression in response to oncogene activity and anti-proliferative signals. Cell Res. 2015;25(11):1205-1218.
18. Abdel-Wahab O, Adli M, Lafave LM, et al. ASXL1 mutations promote myeloid transformation through loss of PRC2-mediated gene repression. Cancer Cell. 2012;22(2):180-193.
19. Abdel-Wahab O, Gao J, Adli M, et al. Deletion of Asxl1 results in myelodysplasia and severe developmental defects in vivo. J Exp Med. 2013;210(12):2641-2659.
20. Guo Y, Zhou Y, Yamatomo S, et al. ASXL1 alteration cooperates with JAK2V617F to accelerate myelofibrosis. Leukemia. 2019;33(5):1287-1291.
21. Arber DA, Orazi A, Hasserjian R, et al. The 2016 revision to the World Health Organization classification of myeloid neoplasms and acute leukemia. Blood. 2016;127(20):2391-2405.
22. Ozono Y, Shide K, Kameda T, et al. Neoplastic fibrocytes play an essential role in bone marrow fibrosis in Jak2V617F-induced primary myelofibrosis mice. Leukemia. 2021;35(2):454-467.
23. Verstovsek S, Manshouri T, Pilling D, et al. Role of neoplastic monocyte-derived fibrocytes in primary myelofibrosis. J Exp Med. 2016;213(9):1723-1740.
24. Tefferi A, Vaidya R, Caramazza D, Finke C, Lasho T, Pardanani A. Circulating interleukin (IL)-8, IL-2R, IL-12, and IL-15 levels are independently prognostic in primary myelofibrosis: a comprehensive cytokine profiling study. J Clin Oncol. 2011;29(10):1356-1363.
25. Koschmieder S, Chatain N. Role of inflammation in the biology of myeloproliferative neoplasms. Blood Rev. 2020;42:100711.
26. Heaton WL, Senina AV, Pomicter AD, et al. Autocrine Tnf signaling favors malignant cells in myelofibrosis in a Tnfr2-dependent fashion. Leukemia. 2018;32(11):2399-2411.
27. Fisher DAC, Miner CA, Engle EK, et al. Cytokine production in myelofibrosis exhibits differential responsiveness to JAK-STAT, MAP kinase, and NFκB signaling. Leukemia. 2019;33(8):1978-1995.
28. Auffray C, Sieweke MH, Geissmann F. Blood monocytes: development, heterogeneity, and relationship with dendritic cells. Annu Rev Immunol. 2009;27:669-692.
29. Domínguez PM, Ardavín C. Differentiation and function of mouse monocyte-derived dendritic cells in steady state and inflammation. Immunol Rev. 2010;234(1):90-104.
30. Locati M, Curtale G, Mantovani A. Diversity, mechanisms, and significance of macrophage plasticity. Annu Rev Pathol. 2020;15:123-147.
31. Chow A, Lucas D, Hidalgo A, et al. Bone marrow CD169+ macrophages promote the retention of hematopoietic stem and progenitor cells in the mesenchymal stem cell niche. J Exp Med. 2011;208(2):261-271.
32. Schneider RK, Mullally A, Dugourd A, et al. Gli1(+) mesenchymal stromal cells are a key driver of bone marrow fibrosis and an important cellular therapeutic target. Cell Stem Cell. 2017;20(6):785-800.
33. Decker M, Martinez-Morentin L, Wang G, et al. Leptin-receptor-expressing bone marrow stromal cells are myofibroblasts in primary myelofibrosis. Nat Cell Biol. 2017;19(6):677-688.
34. Gleitz HFE, Dugourd AJF, Leimkühler NB, et al. Increased CXCL4 expression in hematopoietic cells links inflammation and progression of bone marrow fibrosis in MPN. Blood. 2020;136(18):2051-2064.
35. Asada S, Fujino T, Goyama S, Kitamura T. The role of ASXL1 in hematopoiesis and myeloid malignancies. Cell Mol Life Sci. 2019;76(13):2511-2523.
36. Scheuermann JC, de Ayala Alonso AG, Oktaba K, et al. Histone H2A deubiquitinase activity of the Polycomb repressive complex PR-DUB. Nature. 2010;465(7295):243-247.
37. Krishnaraju K, Hoffman B, Liebermann DA. Early growth response gene 1 stimulates development of hematopoietic progenitor cells along the macrophage lineage at the expense of the granulocyte and erythroid lineages. Blood. 2001;97(5):1298-1305.
38. Yao J, Mackman N, Edgington TS, Fan ST. Lipopolysaccharide induction of the tumor necrosis factor-alpha promoter in human monocytic cells. Regulation by Egr-1, c-Jun, and NF-kappaB transcription factors. J Biol Chem. 1997;272(28):17795-17801.
39. Fleischman AG, Aichberger KJ, Luty SB, et al. TNFα facilitates clonal expansion of JAK2V617F positive cells in myeloproliferative neoplasms. Blood. 2011;118(24):6392-6398.
40. Leimkühler NB, Gleitz HFE, Ronghui L, et al. Heterogeneous bone-marrow stromal progenitors drive myelofibrosis via a druggable alarmin axis. Cell Stem Cell. 2021;28(4):637-652.e638.
41. Yang H, Kurtenbach S, Guo Y, et al. Gain of function of ASXL1 truncating protein in the pathogenesis of myeloid malignancies. Blood. 2018;131(3):328-341.
42. Balasubramani A, Larjo A, Bassein JA, et al. Cancer-associated ASXL1 mutations may act as gain-of-function mutations of the ASXL1-BAP1 complex. Nat Commun. 2015;6:7307.
43. Koschmieder S, Mughal TI, Hasselbalch HC, et al. Myeloproliferative neoplasms and inflammation: whether to target the malignant clone or the inflammatory process or both. Leukemia. 2016;30(5):1018-1024.
44. Zingariello M, Martelli F, Ciaffoni F, et al. Characterization of the TGF-β1 signaling abnormalities in the Gata1low mouse model of myelofibrosis. Blood. 2013;121(17):3345-3363.
45. Kisseleva T, Uchinami H, Feirt N, et al. Bone marrow-derived fibrocytes participate in pathogenesis of liver fibrosis. J Hepatol. 2006;45(3):429-438.
46. Reich B, Schmidbauer K, Rodriguez Gomez M, et al. Fibrocytes develop outside the kidney but contribute to renal fibrosis in a mouse model. Kidney Int. 2013;84(1):78-89.
47. Fursova NA, Turberfield AH, Blackledge NP, et al. BAP1 constrains pervasive H2AK119ub1 to control the transcriptional potential of the genome. Genes Dev. 2021;35(9-10):749-770.
48. Conway E, Rossi F, Fernandez-Perez D, et al. BAP1 enhances Polycomb repression by counteracting widespread H2AK119ub1 deposition and chromatin condensation. Mol Cell. 2021;81(17):3526-3541.